Low-Temperature Photochemistry and Photodynamics of the Chromophore of Green Fluorescent Protein (GFP)

Markus Stübner[†] and Peter Schellenberg*[,‡]

Lehrstuhl für Physik Weihenstephan, Physik-Department E14, TU München, D-85350 Freising, Germany, and Institut für Physikalische und Theoretische Chemie, TU München, D-85747 Garching, Germany

Received: September 20, 2002; In Final Form: December 20, 2002

Hole-burning and temperature-dependent spectroscopy in green fluorescent protein (GFP) have been shown in the literature to be valuable tools in unraveling the photodynamics of this protein. It would be straightforward to perform similar experiments on the isolated GFP chromophore to differentiate between properties that are affiliated with the chromophore itself and those that are rather determined by the protein cage. To this end, we performed temperature-dependent and hole-burning spectroscopy on the organically synthesized chromophore of GFP in alcohol solutions. It can be shown that many of the spectral features described for the GFP protein are also observed in the chromophore dissolved in alcohol and alcohol glasses. In addition to the neutral state A and the anionic state B of the chromophore, additional states (I states) are observed. Analogous to those of the GFP protein, these states are assigned to unrelaxed anionic environments and are distinguished from the relaxed environment by different arrangements of the hydrogen bonds to the matrix. The comparison of the spectroscopic and kinetic properties of the GFP chromophore in alcohol solution with the protein has implications for the understanding of the photodynamics of GFP. We demonstrate that the protein cage alters the properties of the chromophore significantly. In particular, it can be concluded that proton transfer in the protein proceeds along better-defined reaction trajectories compared to those of the chromophore embedded in an amorphous matrix. Furthermore, the electron−phonon coupling of the chromophore of GFP in the amorphous lattice is higher compared to that in the protein, which is indicative of differences in the ground- and excited-state potential surfaces. The protein cage exerts restrictions upon the chromophore that may also be responsible for the high fluorescence quantum yield in the protein even at room temperature.

1. Introduction

Green fluorescent protein (GFP) contains a chromophore that is produced in the protein by the autocatalytic cyclization and oxidation of the three adjacent amino acids Ser65-Tyr66-Gly67 during the folding of the protein.[1−3] The particular protein cage has the shape of a tight barrel formed by 11 β sheets and plays a crucial role in the formation of the chromophore during or shortly after folding. This is also witnessed by the fact that many mutations of Ser65 and Tyr66 also lead to the particular cyclization and oxidation reaction forming a dye. Recently, related proteins from other species of phyllum *Cnidaria*, which exhibit orange and red fluorescence due to an altered chromophore, have also been discovered.[4−8]

Although GFP and its mutants are usually distinguished for their uniqueness as fluorescent probes in cell biology and molecular biology (for reviews, see refs 9−11), they have also turned out to exhibit a puzzling photodynamics that is interesting in its own right. However, this photodynamics can hamper the usability of GFP as a biological probe. A thorough understanding of the underlying processes is therefore crucial.[12]

Wild-type green fluorescent protein (wt-GFP) and some of its mutants show absorption bands with maxima at around 398 and 477 nm,[1,13,14] whose ratios are dependent on environmental parameters such as temperature, pH, ionic strength, and protein concentration.[13,15,16] The two peaks are attributed to the neutral (A form) and the anionic (B form) chromophore, respectively.

It became obvious early on that the protein cage significantly changes the spectral and photodynamic properties of the chromophore. This has been demonstrated by comparing the intact protein with the denatured protein or the free organically synthesized chromophore 4-hydroxybenzylidene-2,3-dimethylimidazolinone (HBDI) in solution.[17] The absorption and emission maxima of the neutral and anionic states in HBDI in alcohol solution are blue-shifted by about 20 nm.

The fluorescence is strongly quenched at room temperature, and the excited-state relaxation is on the order of picoseconds and dependent on the viscosity of the solvent.[18,19] The fluorescence quantum yield rises significantly upon cooling below the glass-transition temperature or by embedding HBDI in a poly(vinyl alcohol) (PVA) film.[20]

Time-resolved spectroscopy experiments led to the postulation of excited-state proton transfer (ESPT),[21,22] which also provided an explanation for the remarkably strong red shift of the fluorescence of wt-GFP by 77 nm relative to absorption. In this picture, the proton is transferred from the phenolic oxygen of the chromophore to the protein lattice during excitation, and the fluorescence emission takes place from the anionic state. Because of the quantitative recovery of the neutral A form, the introduction of a third, unrelaxed anionic form as an intermediate (I form) became necessary. It is understood to be the anionic state of the chromophore in a protein environment similar to

* To whom correspondence should be addressed. E-mail: schelli@imb-jena.de. Present address: Institute of Molecular Biotechnology, Beutenbergstrasse 11, D-07745 Jena, Germany.
† Lehrstuhl für Physik Weihenstephan.
‡ Institut für Physikalische und Theoretische Chemie.

10.1021/jp027038d CCC: $25.00
Published on Web 02/04/2003

the neutral A form. This I form is assumed to be intimately connected to the presence of the particular protein arrangement. X-ray investigations provided a picture in which two different hydrogen bonding networks involving the chromophore and amino acid residues are central to the existence of different forms of the chromophore and to the occurrence of ESPT.[23] Theoretical continuum electrostatics calculations[24] and molecular dynamics simulation studies[25] also support the picture of a changing hydrogen bond network. A recent thorough investigation of the kinetics of GFP indicated that ESPT dominantly occurs from vibrationally unrelaxed states.[26]

Different protonation states for the chromophore in the protein environment have also been proposed on theoretical grounds,[27−29] but can now be excluded on the basis of vibrational studies.[30−32]

Hole-burning experiments on the GFP wild type and mutants gave additional insight into the photophysical behavior of the chromophore in the protein cage. In particular, it could be demonstrated that the I form is also present in wild-type GFP in thermal equilibrium with the B form. At low temperature, the I form eventually vanishes,[33] but it can be produced photochemically by irradiating into the A or B form, giving a thermally stable photoproduct. An even more sophisticated pattern has been described in which hole burning into the A and B bands led to distinct photoproducts identified by their absorption maxima and their thermal recovery pattern in hole-burning experiments.[34] The reaction is photoreversible, and excitation of the I photoproduct delivers A and B. Interestingly, the reaction path that was inhibited is the direct production of B from A and vice versa. An arrangement resembling the I state is also present in some GFP mutants in thermal equilibrium with B or can be produced by a photoreaction and could even be the ground state of the anionic chromophore in some particularly red-shifted mutants.[35]

The existence of additional nonfluorescent states, possibly correlated to the zwitterionic form of the chromophore, has been postulated on the basis of single-molecule spectroscopy. The blinking behavior as well as the light-induced recovery of fluorescence regularly observed in these experiments has been attributed to such dark states.[36−39] Additional confirmation and the determination of multiple time constants depending on the particular mutant came from fluorescence correlation spectroscopy.[40−43] Theoretical models have also been put forward to explain this dynamics.[44]

Apart from the photoreversible reactions, the irradiation of GFP, particularly by UV light at 254 nm, led to the irreversible decarboxylation of a glutamic acid residue.[45]

In this paper, we show that the photophysical properties of the free chromophore are surprisingly similar to those of the chromoprotein. In particular, the anionic B state of the chromophore is in thermal equilibrium with a more red-shifted state, which diminishes as the temperature of the sample is lowered. Upon excitation of the neutral or anionic form, a piling up of photoproduct red shifted from the B form can be observed. Both of these observations are completely analogous to the properties of the GFP protein, and we assume that the additional red-shifted state can be viewed as being similar to the I form in GFP.

2. Experimental Methods

The GFP chromophore 4-hydroxybenzylidene-2,3-dimethylimidazolinone (HBDI) was synthesized according to the literature,[46] and the purity was tested by NMR spectroscopy and by thin-layer chromatography.

HBDI was dissolved in glass-forming alcohols with different glass-transition temperatures and hydrogen bonding strengths such as ethanol/methanol 3:1 (EtOH/MeOH) and *n*-butanol/*t*-butanol l:1 (BuOH). These protic solvent mixtures are known for very good glass-forming properties, allowing for spectroscopic measurements at low temperature. They were also tested before in similar systems such as the dye resorufin,[47,48] cresyl violet,[49] and chinizarin.[50]

The absorption spectra were taken with a Perkin-Elmer Lambda 2S UV/Vis spectrometer set to 2-nm resolution. For recording the spectra at different temperatures, the sample was placed in a 1-mm path-length quartz cuvette and cooled with a Leybold VSL 3-300 flow cryostat using liquid nitrogen.

A Spex Fluorolog with 0.22-m double monochromators and the flow cryostat described above was utilized to take the fluorescence emission and excitation spectra.

The low-temperature photochemistry experiments were performed at 4 K in a homemade helium-bath cryostat. To induce the photoreaction, an excimer laser pumped dye laser (Lambda-Physics LPD 3002E) with a spectral width of 0.15 cm^{-1} was utilized. The pre- and post-burned spectra were taken with a 1-m Jobin Yvon monochromator with a grating blazed at 400 nm in first order. The effective spectral resolution was set to 0.2 cm^{-1}. To achieve a high photoproduct yield, samples with a high optical density at the burning position were used, and the sample was exposed to up to 200 mW/cm^2 for more than 1 h. No efforts were made to prevent saturation and power broadening.

To determine the upper limit for the homogeneous line width, hole-burning experiments were done using the excimer laser pumped dye laser with an etalon placed in the cavity, which narrowed the optical width to 0.04 cm^{-1}. The burning intensity was varied between 0.05 and 5 mW/cm^2 with burning times of several minutes. Scanning was performed by frequency tuning of the laser, with a maximal range of about 24 cm^{-1}. No zero-phonon holes could be observed at any wavelength; the irradiation caused only a lowering of the optical density over the whole detection range.

Temperature-cycling experiments were done in a Leybold-Heraeus flow cryostat cooled with liquid helium. Briefly described, the sample was cooled to the burning temperature of 4.0 K, at which it was submerged in liquid helium. For cycling, the sample temperature was raised to 4.5 K, and the spectra were taken. The sample was then heated to an excursion temperature, cooled to 4.5 K, and the spectrum was scanned again. This procedure was repeated for increasingly higher temperatures, and the back reaction was recorded by integrating numerically over the area of the photoproduct. Note that this is a modification of the common temperature-cycling protocol in which burning and spectral detection temperatures are identical. In this way, efficient coupling to the heat bath at the utilized high light doses during burning and a good optical quality of the sample during detection are ensured. The return to the temperature at which the photoproduct spectrum was recorded was done to exclude a temperature drift of the spectral baseline.

The data were fitted by assuming a Gaussian distribution of barrier heights, which is typical for photochemical hole-burning reactions. For the fitting procedure, a script written in the Matlab clone language Octave was used.

3. Results

The spectrum of HBDI is strongly solvent- and temperature-dependent. Figure 1 shows the temperature dependence of HBDI in neutral EtOH/MeOH (3:1) (A form). Emerging vibrational fine structure is observed upon cooling, as well as a modest

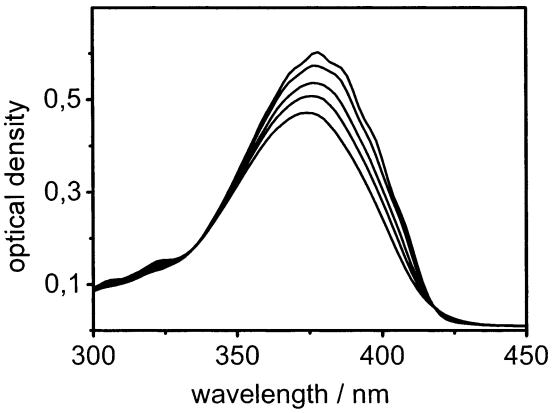

Figure 1. Absorption spectrum of HBDI, neutral form (A) in EtOH/MeOH (3:1), at various temperatures ranging from 80 to 260 K. The optical density decreases with increasing temperature, and the spectrum loses structure.

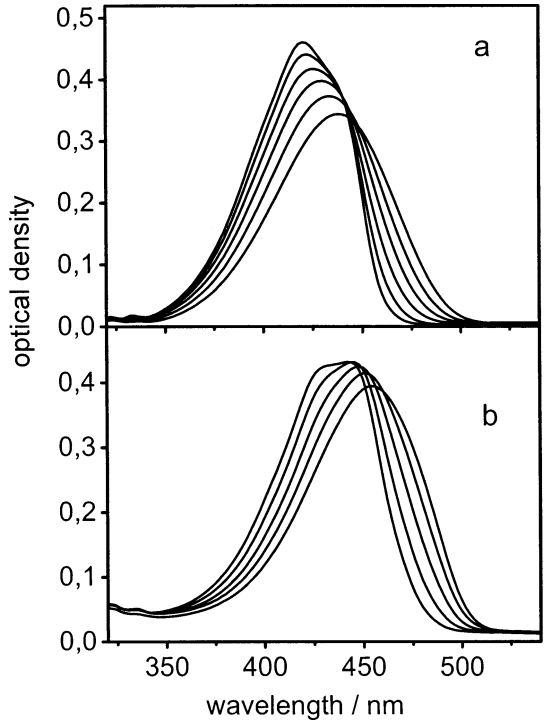

Figure 2. Absorption spectrum of the anionic form of HBDI in EtOH/MeOH (a) and in BuOH (b) at various temperatures. A red-shifted band vanishes with decreasing temperature. An isosbestic point is clearly visible in a, whereas it is smeared out in b.

narrowing of the inhomogeneously broadened band, but hardly any spectral shift of the absorption band.

This spectral property is dramatically changed in the anionic molecule (Figure 2a) prepared by the addition of potassium phosphate to a concentration of 0.05 mol/L to the solvent: A clear change in the absorption spectrum upon cooling, particularly a shift and a narrowing of the absorption band, takes place. The strong change in the red wing of the spectrum and the presence of an isosbestic point can be interpreted as the change of equilibrium and the eventual vanishing of a thermodynamically disfavored absorber. No further alterations in the spectrum can be observed below the glass-transition temperature. The presence of an additional red-shifted anionic state may be interpreted as the analogue to the I state in the GFP protein, which exhibits a comparable pattern of temperature dependency. Similar behavior can be seen in HBDI dissolved in BuOH made alkaline by the addition of 0.03 mol/L of potassium phosphate

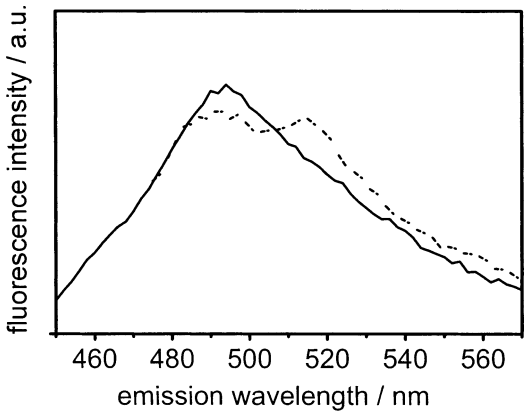

Figure 3. Fluorescence spectra taken at 80 K of HBDI in alkaline BuOH upon excitation at 410 nm (—) and 470 nm (•• ••). Note that at excitation wavelengths larger than 470 nm the fluorescence spectrum exhibits a double-peak structure.

as demonstrated in Figure 2b. Note that the B state is shifted further to the red compared to EtOH/MeOH and that the absorption of the I state is less separated from B. Nevertheless, the fluorescence spectrum of HBDI in alkaline BuOH at 80 K directly demonstrates the presence of the I state in this solvent (Figure 3). Upon excitation at wavelengths greater than 475 nm, the fluorescence spectrum shows a double-peak structure, with the two peaks representing the B and I environments. A similar experiment in EtOH/MeOH did not give any indication of fluorescence from I, likely because it vanishes above the glass-transition temperature of the solvent.

Figure 4 shows the low-temperature absorption spectrum of the chromophore in neutral EtOH/MeOH (3:1) after increasing burning times at 400 nm and the corresponding difference spectrum. There is a strong building up of photoproduct in the range between 450 and 520 nm, spanning the spectral range of the B and I.

Likewise, the anionic form dissolved in weakly alkaline EtOH/MeOH prepared by adding TRIS to a concentration of 0.05 mol/L shows a spectral increase of photoproduct in the range of 490−510 nm (I form) and in the range around 380 nm (A form) after burning into the B band at 445 nm, as shown in Figure 5. Note that the spectral range of the photoproduct extends less to the red than in the neutral form of HBDI (Figure 4), which hints at different photoproducts upon burning into A and B. If a corresponding experiment is performed with a strongly alkaline matrix prepared by adding 2% potassium hydroxide to EtOH/MeOH, then the photoproduct almost exclusively piles up in the spectral range of I but not in the absorption region of A (spectra not shown).

The photoproduct band shows some striking spectral features and is far from smooth. To demonstrate that these features originate from different photoproducts and not from vibrational fine structure, we performed temperature-cycling experiments of the photoproduct after burning in the spectral region of B. Such a temperature-cycling experiment delivers the mean barrier and distribution for the thermally induced back reaction of the photoproduct in question.[51,52] Distinct photoproducts should be correlated to different barriers. The data convincingly show different recovery temperatures after integrating over the spectral ranges indicated in Figure 6. The integration ranges were selected according to the assumed maxima of the individual photoproducts, with the overlap areas dismissed. The fit results are listed in Table 1. Although the center value for the recovery temperature varies by a factor of 2, the width (fwhm) representing the inhomogeneity is almost the same for all of the

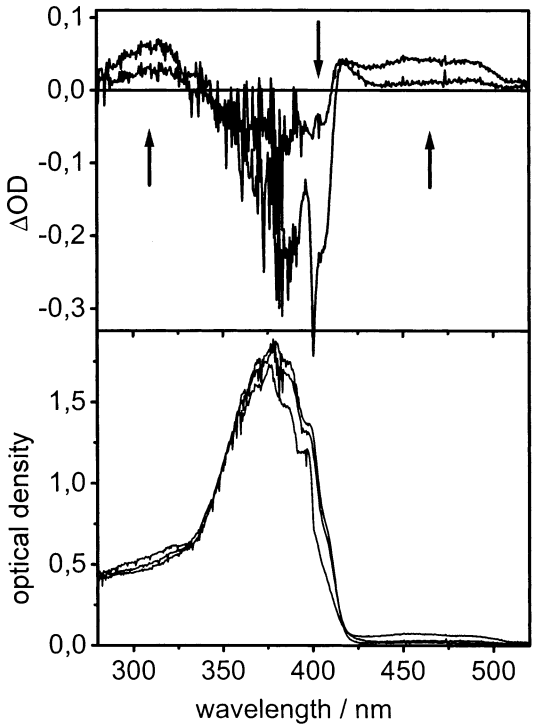

Figure 4. Preburn and photoproduct spectra of neutral HBDI in EtOH/MeOH after burning with various amounts of energy. The burning was done at 400 nm with irradiation times of 1800 and 4800 s at approximately 100 mW/cm^2. The corresponding optical difference spectra are depicted in the upper panel. To get a reasonable amount of photoproduct, a sample with a high optical density in the educt range was used, which caused a large amount of noise in this region, as can be seen in the difference spectra. The pilling up of photoproduct is clearly visible around 440−520 nm and below 330 nm. The increase and decrease in optical density are indicated by arrows.

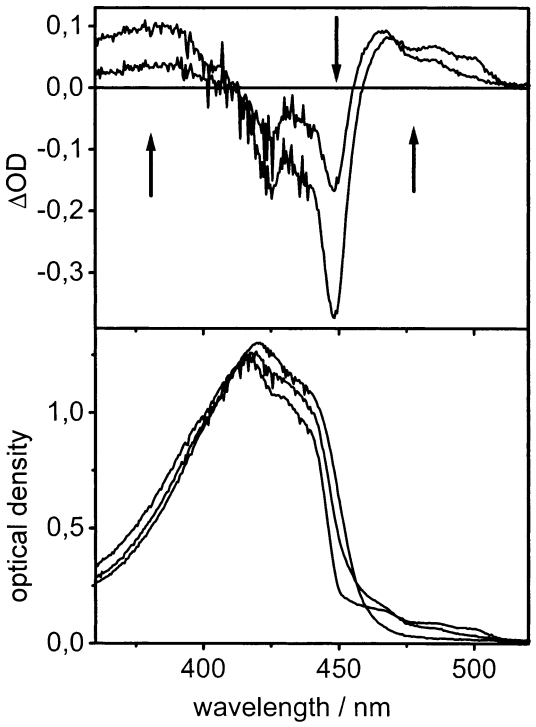

Figure 5. Preburn and photoproduct spectra of anionic HBDI in EtOH/MeOH after burning with various amounts of energy. The burning was done at 445 nm with irradiation times of 900 and 1800 s at approximately 50 mW/cm^2. The optical difference spectra are also shown. Again, the sample has a high optical density in the educt range to be able to produce a reasonable amount of photoproduct. The increase and decrease in optical density are indicated by arrows.

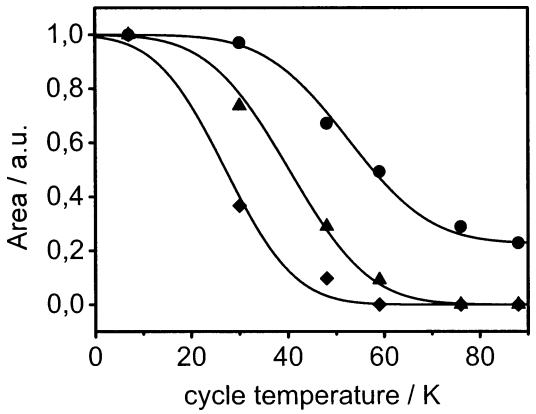

Figure 6. Recovery of photoproduct for the anionic form for different integration ranges: 460−470 nm (●), 480−490 nm (▲), and 500−510 nm (♦). The fits have been made by assuming a Gaussian barrier distribution, and the results are given in Table 1.

photoproduct forms. The recovery of two of the bands is complete, but there is an approximately 20% residual area left at the glass-transition temperature for the band between 460 and 470 nm. Obviously, two distinct photoreactions, one of which is irreversible up to this temperature, are observed.

Extensive efforts were made to burn narrow Lorentzian-shaped holes, which are caused by the excitation of the zero-phonon line of the absorber. Particular attention was given to the red wing of the spectrum, where the relative amount of zero-phonon-line absorption compared to phonon side-wing absorption is largest. In this range, narrow holes can clearly be observed in the GFP protein despite the relatively strong electron−phonon coupling in that system.[33,34] Contrary to the protein, holes cannot be observed even far into the red in HBDI in any of the solvents used. We therefore assume that the electron−phonon coupling in the chromophore in solution is considerably higher than in the protein.

4. Discussion

I. Photodynamics and Photochemistry. By analogy to other photochemical hole-burning reactions, it can be assumed that the low-temperature photochemistry of HBDI in alcohol glasses is governed by a change in the hydrogen bonding network that couples the chromophore to the environment.[47,48,50] The specific temperature dependence of the optical spectrum in connection with the appearance of a photoproduct peak in the spectral range of the thermally disfavored form has been interpreted for other chromophores in alcohol matrices as a change of the hydrogen bonding network. The barrier heights for the thermally induced back reactions were also of the same magnitude in these systems,[48] further supporting a close relationship with the phototransformation in HBDI.

TABLE 1: Gaussian Barrier Distribution Function Parameters for the Thermally Induced Back Reaction for the Distinct Photoproducts in the I Range of the Spectrum

integration range/nm	center/K	width/K
460−470	52.5	32.0
480−490	40.2	30.9
500−510	26.9	27.8

In this work, we establish that HBDI in alcohol solutions shows similar spectral and photochemical reaction behavior to that of the chromophore embedded in the protein cage.[33,34] Specifically, the temperature dependence of the absorption

spectrum led to the conclusion that there is a third state present in thermal equilibrium with the anionic state B, which we assume to be analogous to the I form in the protein. This form can also be produced photochemically at low temperature by light deposition into the A and B bands, parallel to the observed pattern in the protein. Close inspection of the photoproduct range in combination with temperature-cycling experiments reveals a sophisticated pattern of photoproducts that can be compared to that observed for the chromophore in the protein.[34]

Surprisingly, those properties that distinguish GFP, namely, ESPT and the high fluorescence quantum yield even at ambient temperature, cannot be observed in the free chromophore. The free chromophore exhibits only very weak fluorescence at room temperature, albeit the quantum yield increases to values comparable to those of the protein upon cooling of the chromophore below the glass-transition temperature of the matrix. This observation is attributed to the inhibition of the rapid internal conversion of the chromophore in the solid state.[18]

Whereas the nature of the spectral features A and B as the neutral and anionic states of the chromophore is fairly settled, the structure of the unrelaxed intermediate I is still elusive. Originally, it has been postulated to explain the photokinetics of the GFP protein.[21,22] According to these results, B corresponds to the relaxed anionic environment of the GFP chromophore, whereas I, despite being negatively charged, is situated in a solvent cage similar to that of the neutral state A. This unrelaxed form then transforms back into A and only with a very low probability interconverts to B.

The I form appears in different mutants of GFP with the chromophore embedded into altered protein cages. It has also been postulated that it is the stable ground state in some particularly red-shifted mutants such as yellow fluorescent protein.[35]

On the basis of the X-ray structure, it has been suggested that the B form has three hydrogen bonds from the phenylic oxygen to the protein lattice, whereas there are only two hydrogen bonds present in the I form.[23] Earlier work on other chromophores demonstrates that differences in the hydrogen bonding network can account for the observed spectral shifts, the temperature dependence of the spectra, and the photochemistry.[47,48,50] We therefore conclude that the spectral and photodynamic properties of HBDI in alcohol solution and of GFP are mostly governed by alterations of the hydrogen bonding network. Because of the less-restricted solvent cage, HBDI in alcohol solution may form additional hydrogen bonds that are not accessible to the chromophore in the protein.

Indications for an even more complicated binding network in the protein arise from the fact that phototransformations of A and B in the protein lead to different photoproducts, with those of the A form more red-shifted than that of the B form.[34] Again, this is parallel to the observations described here for the free chromophore.

The structure of the photoproduct band also suggests the formation of multiple distinguished forms upon irradiation. This assumption could be confirmed with temperature-cycling spectroscopy, which has the potential of measuring the mean value and the distribution of reaction barriers.[51,52] Briefly described, after producing the photoproduct at a burning temperature T_b, the sample is heated to an excursion temperature T_{ex} and retained there for a waiting time to ensure temperature equilibration. Then, the sample is cooled to T_b again, and the spectrum is taken. This procedure is repeated for increasingly higher excursion temperatures. After each cycle, the remaining amount of photoproduct is determined from the spectral changes by integration over the photoproduct range. All barriers up to T_{ex} can be crossed at each particular cycle, and the amount of photoproduct diminishes accordingly. Assuming an activated process, the maximum barrier height V_T that can be crossed at a certain T_{ex} is[51]

$$V_T = k_b T_{ex} \ln(R_0 \tau) \tag{1}$$

with the preexponential R_0 and the experimental time τ, which is mostly the waiting time at the excursion temperature. We can define a marginal barrier V_m that cannot be crossed at the respective excursion temperature. All molecules at sites with lower barriers have crossed back to the educt state, whereas those with higher barriers are still in the photoproduct state. The number of barriers crossed during the waiting time at the excursion temperature has to be neglectable, which is assured when dealing with a broad distribution of barriers.

The photoproduct area A_p remaining after such a cycle is proportional to the number of unrelaxed molecules[51]

$$A_p \approx \int_{V_m}^{\infty} P_V(V)\, dV \tag{2}$$

$P_V(V)$ is the barrier distribution function. For a reaction with a well-defined reaction coordinate, a Gaussian distribution of reaction barriers can be assumed.[52]

According to eq 1, there is an ambiguity to which the extent the experimental results are determined by the energy barrier V or the kinetic preexponential R_0. It is often assumed that this attempt frequency is on the order of 10^{12} s^{-1}.[34,51] Because of its logarithmic dependence, a small variation in R_0 does not influence the results very much. However, dramatically lower values for R_0 are possible if the reaction involves concerted steps along several system coordinates.[53] In that case, a high negative activation entropy scales down the preexponential, which leads to a higher recovery temperature.

It is notable that although the patterns for the thermally induced back reaction are similar for the GFP protein and for the free chromophore the recovery temperatures are generally higher in the protein.[34] Since ESPT and likely the thermally activated back reaction involve concerted proton-transfer steps in GFP, the higher recovery temperature could indeed be due to a lower preexponential. The higher disorder in the amorphous alcohol glass leads to more possible reaction paths for the proton back reaction and hence to a larger number of accessible states around the activation barrier. Under the assumption of an equal reaction barrier in the protein environment and in alcohol solution, one would need a reduction for the preexponential frequency factor by 6 orders of magnitude compared to that of the chromophore in frozen solution whereas only a reduction of the barrier height by a factor of 2 would be sufficient. On first sight, this estimation hints to a lowering of the activation barrier as the primary cause for the observed deviation between protein and solution. However, even a reduction of the preexponential factor by 9 orders of magnitude has been observed in a concerted proton tautomerization reaction in a porphine-type system,[53] and global conformational fluctuations of a protein are correlated to a preexponential of only 10^6 s^{-1}.[54] Therefore, we believe that the contribution of a small preexponential to the observed lower recovery temperature in an amorphous matrix is a reasonable assumption.

The observation of ESPT in the protein and its absence in the chromophore in solution are also consistent with this picture. A significantly narrowed distribution of reaction trajectories in

the protein would lead to efficient proton transfer and back transfer without much dissipation of energy along reaction coordinates not involving ESPT and ground-state proton back transfer. We suggest a protein cage that shapes the potential surfaces in such a way that concerted proton transfer via an eleborate network of hydrogen bonds is optimized. The thermally activated back-reaction kinetics probed in temperature-cycling experiments progresses on the ground-state potential surface, whereas ESPT takes place on the excited-state potential surface. Nevertheless, we believe that the arguments that are valid for the ground-state properties can equally be applied to proton transfer on the excited-state potential surface.

The photoproduct area closest to the B band in the anionic HBDI contains a contribution that is irreversible up to the glass-transition temperature. The underlying mechanism for this phototransformation is probably not related to a rearrangement of H bonds but instead could be a cis−trans isomerization reaction of the hula-twist motion type.[44] Alternatively, a metastable zwitterionic form can also not be excluded.[36,37,44]

II. Homogeneous Line Width and Electron−Phonon Coupling. In the GFP protein, the burning of narrow holes (zero-phonon-line holes) is limited to the red wing of the absorption spectrum for either protonation state, whereas the blue part of the spectrum is solely attributed to absorption via molecular vibrational and lattice phonon levels coupled to the electronic transition.[33,34] This is indicative of a relatively strong electron−phonon coupling. Following the experiments done in this work, narrow holes could neither be burned in the neutral nor in the anionic band of HBDI in frozen alcohol solution at any wavelength. This observation is obviously not due to a lack of photochemical reaction paths since broadly structured photochemical transformations can be observed in the spectrum. Accordingly, we have to conclude that the inability to burn narrow holes in the inhomogeneously broadened absorption band is due to a very strong electron−phonon coupling.

A large coupling of the molecular and solvent cage vibrational modes to the electronic transition originates from a large difference in the nuclear coordinates between the ground state and first excited state. In this case, the nuclear coordinates after excitation are far from their equilibrium positions, and a considerable vibrational relaxation has to take place. This argument applies to the molecular vibrational modes as well as to the phonon modes of the amorphous or protein lattice since a large displacement of molecular coordinates usually implies large relocations within the solvent cage.

The strength of the electron−phonon coupling in the GFP chromophore could arise from a large torsion angle of the C═C double bond upon excitation or from the strong charge-transfer (CT) character of the electronic transition.

The ground- and excited-state equilibrium geometries of the chromophore have been determined by quantum mechanical calculations.[44,55] These show that the chromophore is basically planar in the ground state for the neutral as well as the anionic form, although the location of the exocyclic double bond is partially interchanged in the anion because of the chinoid character of the phenolic ring. In the excited state, the angle around the exocyclic double bond is close to 90°.[44,55] However, steric effects imposed by the environment have to be included when dealing with the chromophore embedded in the protein or the amorphous lattice, and the energetic minimum of the excited-state potential surface may be shifted to torsion angles considerably smaller than 90°.[56] A large change of the double-bond torsional angle between the ground state and first excited state leads to strong electronic−vibrational coupling since the excited-state equilibrium geometry is very different from the ground-state geometry, and the system ends up in a vibrationally unrelaxed excited state. Similarly, the solvent/protein cage has to readjust considerably, giving a strong phonon contribution. This could be the reason for the already relatively strong vibrational coupling to the electronic transition in the protein. Restrictions imposed upon the chromophore from the protein cage diminish the difference between the equilibrium geometries of the ground state and first excited state compared to that of the amorphous lattice while rationalizing the weaker electron−phonon coupling. A model postulating differences in the excited-state potential surfaces between the chromophore embedded in the protein cage and in solution has been deducted from resonance Raman experiments.[32]

A reduction of the electron−phonon coupling in the protein compared to HBDI in the amorphous lattice can also originate from the difference in the charge-transfer (CT) character of the electronic transition. A CT transition leads to strong electron−phonon coupling since the interaction potentials between the chromophore and matrix change considerably upon excitation, which causes a large shift of the excited-state potential surface.

Theoretical calculations indicate that the anion of HBDI exhibits zwitterionic character in the excited state, whereas the charges are less separated in the ground state.[57] This is in line with Stark experiments on GFP[21,58] that show strong CT character of the transition in the anionic chromophore. Because of the fixed position of the hydrogen bonding network or the electrostatic properties of the protein cage, the zwitterionic character in the excited state may be diminished in the protein, and the electron−phonon coupling would be weaker. However, the charge-transfer character of neutral HBDI is reported to be smaller, and if the electron−phonon coupling originated from CT, one should expect to get a smaller electron−phonon coupling in neutral HBDI, which has not been observed. Therefore, a strong CT character as the sole origin of the observed strong electron−phonon coupling can be excluded.

The strong vibrational coupling to the electronic transition of the chromophore of GFP gained additional importance following the postulation that ESPT occurs from the vibrationally unrelaxed excited state;[26] therefore, strong electron−phonon coupling is a prerequisite for the high quantum yield of ESPT in GFP. Nevertheless, the absence of ESPT in HBDI despite the even higher vibrational coupling in an alcoholic glass gives evidence that other factors are equally necessary requirements for observing ESPT, namely, an optimized solvent cage and protein environment.

5. Conclusions

The presented work provides evidence that the spectroscopic and photochemical properties of GFP previously ascribed to a sophisticated interrelation between the chromophore and the surrounding protein cage can also be observed in the chromophore in solution. This is particularly evidenced by the appearance of a thermally disfavored form of the anionic state of the chromophore (I state) in equilibrium with the ground state (B state). Analogously to GFP, the absorption band of the I state is red shifted relative to that of the anionic ground state. The photoproduction of a manifold of metastable states and their thermally induced recovery kinetics indicate that the stabilization of these states is not solely due to the protein cage. We postulate that the complex absorption-band structure and photochemistry are caused by changes in the hydrogen bonding network between the chromophore and the protein.

Despite the similarities with respect to spectral and photochemical properties, we detect clear differences between the

protein and amorphous glass that are due to restraints imposed on the chromophore by the preshaped environment of the protein cage. By comparing the electron−phonon coupling in the protein and in the amorphous lattice, we show that the ground- and excited-state potential surfaces of the chromophore are altered considerably by the protein environment. Even though the recovery kinetics for the metastable photoproducts is qualitatively similar in the protein and the amorphous host, the thermally induced back reactions occur at lower temperatures in the amorphous host compared to those in the protein. We conclude that the proton-transfer reaction back to the educt state progresses along better-defined trajectories in the protein compared to those in the amorphous matrix. Although only the ground-state reaction kinetics can be probed in thermal recovery experiments, the picture of proton transfer along well-defined reaction trajectories can likely be applied to the excited state. It would be a reasonable explanation for the high quantum yield for ESPT in the protein, whereas this process cannot be observed in the amorphous host.

Acknowledgment. We acknowledge the support of Professors M.-E. Michel-Beyerle and J. Friedrich, Technical University Munich. The dye HBDI used in this investigation was synthesized by P.S. during his stay in the group of Professors V. Nagarajan and W. W. Parson at the Department of Biochemistry, University of Washington, Seattle. I appreciate the encouragement and useful discussions of V. Helms, A. Voityuk, and C. Scharnagl, and I thank S. Meech for sending a preprint of his work. This work was financed by the DFG, SFB533 Lichtinduzierte Dynamik von Biopolymeren.

References and Notes

(1) Heim, R.; Prasher, D. C.; Tsien, R. Y. *Proc. Natl. Acad. Sci. U.S.A.* **1994**, *91*, 12501.
(2) Cody, C. W.; Prasher, D. C.; Westler, W. M.; Prendergast, F. G.; Ward, W. W. *Biochemistry* **1992**, *32*, 1212.
(3) Nishiuchi, Y.; Inui, T.; Nishio, H.; Bodi, J.; Kimura, T.; Tsuji, F. I.; Sakakibara, S. *Proc. Natl. Acad. Sci. U.S.A.* **1998**, *95*, 13549.
(4) Matz, M. V.; Fradkov, A. F.; Labas, Y. A.; Savitsky, A. P.; Zaraisky, A. G.; Markelov, M. L.; Lukyanov, S. A. *Nat. Biotechnol.* **1999**, *17*, 969.
(5) Gross, L. A.; Baird, G. S.; Hoffman, R. C.; Baldridge, K. K.; Tsien, R. Y. *Proc. Natl. Acad. Sci. U.S.A.* **2000**, *97*, 11990.
(6) Heikal, A. A.; Hess, S. T.; Baird, G. S.; Tsien, R. Y.; Webb, W. W. *Proc. Natl. Acad. Sci. U.S.A.* **2000**, *97*, 11996.
(7) Wall, M. A.; Socolich, M.; Ranganathan, R. *Nat. Struct. Biol.* **2000**, *7*, 1133.
(8) Labas, Y. A.; Gurskaya, N. G.; Yanushevich, Y. G.; Fradkov, A. F.; Lukyanov, K. A.; Lukyanov, S. A.; Matz, M. V. *Proc. Natl. Acad. Sci. U.S.A.* **2002**, *99*, 4256.
(9) Tsien, R. Y. *Annu. Rev. Biochem.* **1998**, *67*, 509.
(10) Chalfie, M.; Kain, S. *Green Fluorescent Protein: Properties, Applications, and Protocols*; Wiley-Liss: New York, 1998.
(11) *Green Fluorescent Proteins;* Sullivan, K. F., Kay, S. A., Eds.; Methods in Cell Biology; Academic Press: San Diego, CA, 1999; Vol. 58.
(12) Zumbusch, A.; Jung, G. *Single Mol.* **2000**, *1*, 261.
(13) Ward, W. W.; Prentice, H. J.; Roth, A. F.; Cody, C. W.; Reves, S. C. *Photochem. Photobiol.* **1982**, *35*, 803.
(14) Palm, G. J.; Zdanov, A.; Gaitanaris, G. A.; Stauber, R.; Pavlakis, G. N.; Wlodawer, A. *Nat. Struct. Biol.* **1997**, *4*, 361.
(15) Elsliger, M.-A.; Wachter, R. M.; Hanson, G. T.; Kallio, K.; Remington, S. J. *Biochemistry* **1999**, *38*, 5296.
(16) Cubitt, A. B.; Heim, R.; Adams, S. R.; Boyd, A. E.; Gross, L. A.; Tsien, R. Y. *Trends Biochem. Sci.* **1995**, *20*, 448.
(17) Niwa, H.; Inouye, S.; Hirano, T.; Matsuno, T.; Kojima, S.; Kubota, M.; Ohashi, M.; Tsuji, F. I. *Proc. Natl. Acad. Sci. U.S.A.* **1996**, *93*, 13617.
(18) Webber, N. M.; Litvinenko, K. L.; Meech, S. R. *J. Phys. Chem. B* **2001**, *105*, 8036.
(19) Litvinenko, K. L.; Webber, N. M.; Meech, S. R. *Bull. Chem. Soc. Jpn.* **2002**, *75*, 1.
(20) Mayer, E.; Davies, B. P.; Schellenberg, P. Unpublished results.
(21) Chattoraj, M.; King, B. A.; Bubliz, G. U.; Boxer, S. G. *Proc. Natl. Acad. Sci. U.S.A.* **1996**, *93*, 8362.
(22) Lossau, H.; Kummer, A.; Heinecke, R.; Pöllinger-Dammer, F.; Kompa, C.; Bieser, G.; Jonsson, T.; Silva, C. M.; Yang, M. M.; Youvan, D. C.; Michel-Beyerle, M.-E. *Chem. Phys.* **1996**, *213*, 1.
(23) Brejc, K.; Sixma, T. K.; Kitts, P. A.; Kain, S. R.; Tsien, R. Y.; Ormö, M.; Remington, S. J. *Proc. Natl. Acad. Sci. U.S.A.* **1997**, *94*, 2306.
(24) Scharnagl, C.; Raupp-Kossmann, R.; Fischer, S. F. *Biophys. J.* **1999**, *77*, 1839.
(25) Lill, M. A.; Helms, V. *Proc. Natl. Acad. Sci. U.S.A.* **2002**, *99*, 2778.
(26) Winkler, K.; Lindner, J.; Subramaniam, V.; Jovin, T. M.; Vöhringer, P. *Phys. Chem. Chem. Phys.* **2002**, *4*, 1072.
(27) Voityuk, A. A.; Michel-Beyerle, M.-E.; Rösch, N. *Chem. Phys. Lett.* **1997**, *272*, 162.
(28) Yazal, J.; Prendergast, F. G.; Shaw, D. E.; Pang, Y.-P. *J. Am. Chem. Soc.* **2000**, *122*, 11411.
(29) Voityuk, A. A.; Kummer, A. D.; Michel-Beyerle, M.-E.; Rösch, N. *Chem. Phys.* **2001**, *269*, 83.
(30) Van Thor, J. J.; Pierik, A. J.; Nugteren-Roodzant, I.; Xie, A.; Hellingwerf, K. J. *Biochemistry* **1998**, *37*, 16915.
(31) Bell, A. F.; He, X.; Wachter, R. M.; Tong, P. J. *Biochemistry* **2000**, *39*, 4423.
(32) Schellenberg, P.; Johnson, E.; Esposito, A.; Reid, P.; Parson, W. W. *J. Phys. Chem. B* **2001**, *105*, 5316.
(33) Creemers, T. M. H.; Lock, A. J.; Subramaniam, V.; Jovin, T. M.; Völker, S. *Nat. Struct. Biol.* **1999**, *6*, 557.
(34) Seebacher, C.; Deeg, F. W.; Bräuchle, C.; Wiehler, J.; Steipe, B. *J. Phys. Chem. B* **1999**, *103*, 7728.
(35) Kummer, A. D.; Wiehler, J.; Rehaber, H.; Kompa, C.; Steipe, B.; Michel-Beyerle, M. E. *J. Phys. Chem. B* **2000**, *104*, 4791.
(36) Dickson, R. M.; Cubitt, A. B.; Tsien, R. Y.; Moerner, W. E. *Nature (London)* **1997**, *388*, 355.
(37) Jung, G.; Wiehler, J.; Gohde, W.; Tittel, J.; Basche, T.; Steipe, B.; Bräuchle, C. *Bioimaging* **1998**, *6*, 54.
(38) Garcia-Parajo, M. F.; Segers-Nolten, G. M. J.; Veerman, J.-A.; Greve, J.; Van Hulst, N. F. *Proc. Natl. Acad. Sci. U.S.A.* **2000**, *97*, 7237.
(39) Jung, G.; Mais, S.; Zumbusch, A.; Bräuchle, C. *J. Phys. Chem. A* **2000**, *104*, 873.
(40) Haupts, U.; Maiti, S.; Schwille, P.; Webb, W. W. *Proc. Natl. Acad. Sci. U.S.A.* **1998**, *95*, 13573.
(41) Widengren, J.; Mets, Ü.; Rigler, R. *Chem. Phys.* **1999**, *250*, 171.
(42) Widengren, J.; Terry, B.; Rigler, R. *Chem. Phys.* **1999**, *250*, 259.
(43) Schwille, P.; Kummer, S.; Heikal, A. A.; Moerner, W. E.; Webb, W. W. *Proc. Natl. Acad. Sci. U.S.A.* **2000**, *97*, 151.
(44) Weber, W.; Helms, V.; McCammon, J. A.; Langhoff, P. W. *Proc. Natl. Acad. Sci. U.S.A.* **1999**, *96*, 6177.
(45) Van Thor, J. J.; Gensch, T.; Hellingwerf, K. J.; Johnson, L. N. *Nat. Struct. Biol.* **2002**, *9*, 37.
(46) Kojima, S.; Ohkawa, H.; Hirano, T.; Maki, S.; Niwa, H.; Ohashi, M.; Inouye, S.; Tsuji, F. I. *Tetrahedron Lett.* **1998**, *39*, 5239.
(47) Van den Berg, R.; Völker, S. *Chem. Phys.* **1988**, *128*, 257.
(48) Schellenberg, P.; Friedrich, J. *J. Lumin.* **1993**, *56*, 143.
(49) Carter, T. P.; Fearey, B. L.; Hayes, J. M.; Small, G. J. *Chem. Phys. Lett.* **1983**, *102*, 272.
(50) Friedrich, J.; Haarer, D. *Angew. Chem., Int. Ed. Engl.* **1984**, *23*, 257.
(51) Köhler, W.; Friedrich, J. *Phys. Rev. Lett.* **1987**, *59*, 2199.
(52) Schellenberg, P.; Friedrich, J. *J. Chem. Phys.* **1991**, *95*, 189.
(53) Schellenberg, P.; Friedrich, J.; Kikas, J. *J. Chem. Phys.* **1994**, *101*, 9262.
(54) Leeson, D. T.; Wiersma, D. A. *Nat. Struct. Biol.* **1995**, *2*, 848.
(55) Voityuk, A. A.; Michel-Beyerle, M.-E.; Rösch, N. *Chem. Phys. Lett.* **1998**, *296*, 269.
(56) Chen, M. C.; Lambert, C. R.; Urgitis, J. D.; Zimmer, M. *Chem. Phys.* **2001**, *270*, 157.
(57) Scharnagl, C. Personal communication.
(58) Bublitz, G.; King, B.; Boxer, S. G. *J. Am. Chem. Soc.* **1998**, *120*, 9370.